

PHYSICAL REVIEW B

SOLID STATE

THIRD SERIES, VOL. 8, No. 1

1 JULY 1973

ESR Analysis of Pb^{3+} Ions in $Y_3Ga_5O_{12}$

B. Andlauer and J. Schneider

Institut für Angewandte Festkörperphysik der Fraunhofer-Gesellschaft, D 78 Freiburg i.Br., Eckerstrasse 4, Germany

W. Tolksdorf

Philips Forschungslaboratorium GmbH, D 2 Hamburg 54, Germany

(Received 16 February 1973)

Trivalent lead impurity ions $5d^{10}6s^1$ have been detected by electron-spin resonance (ESR) to occur in diamagnetic garnet crystals of $Y_3Ga_5O_{12}$ which were grown from a $PbO-PbF_2$ based flux. From the observed weak anisotropy of the Pb^{207} hyperfine interaction, it could be positively established that the Pb^{3+} ions occupy the dodecahedral sites in the garnet lattice. Trivalent lead impurity ions were also found to occur in the other diamagnetic garnet hosts, $Y_3Al_5O_{12}$, $Lu_3Ga_5O_{12}$, and $Lu_3Al_5O_{12}$.

I. INTRODUCTION

$PbO-PbF_2$ flux growth is a standard technique to synthesize single crystals of diamagnetic and ferrimagnetic garnets, as $Y_3Ga_5O_{12}$ (YGaG) and $Y_3Fe_5O_{12}$ (YIG). Consequently, such flux-grown garnet single crystals are liable to be contaminated with traces of the flux constituents, as lead and fluorine. So far, little is known about the way such inevitable impurities are incorporated into the garnet lattice and about their potential influence on the magnetic properties of ferrimagnetic garnets, as YIG.

In this paper, an electron-spin-resonance (ESR) analysis of lead impurity ions in the diamagnetic garnet YGaG will be presented. This analysis will reveal that a certain amount of the lead impurity ions is present in the somewhat unusual trivalent paramagnetic charge state Pb^{3+} , $5d^{10}6s^1$. Chemical identification of the paramagnetic center ascribed to lead is rendered unambiguous by the observation of characteristic hyperfine-structure satellites in the ESR spectrum. These arise from the only stable lead isotope having nuclear spin, i. e., Pb^{207} , 20.8 at.%, $I = \frac{1}{2}$. The magnitude of the Fermi-type hyperfine interaction was found to be considerable, as expected for an unpaired 6s electron. It is comparable with the energy of the microwave quantum. Consequently, full use of the

Breit-Rabi equations is compulsory for an interpretation of the ESR spectra. Occasionally, an angular variation of a Pb^{207} hyperfine signal was observed upon rotating the crystal in the static magnetic field. From this angular dependence it can be unambiguously concluded that the Pb^{3+} ions occupy the rare-earth c sites in the garnet lattice, which have orthorhombic symmetry.

These dodecahedral c sites are surrounded by eight oxygen ligands. Thus, it is helpful to remember that the same coordination is present in thorium oxide ThO_2 , which occurs in the fluorite lattice. The ESR of Pb^{3+} ions in flux-grown ThO_2 single crystals has been previously reported^{1,2}; the Pb^{207} hyperfine-coupling constant was determined as 1.23 cm^{-1} , or 36.9 GHz. The corresponding experimental value to be reported in this paper for YGaG does not greatly differ from the ThO_2 value. This shows that the Pb^{207} hyperfine-coupling constant is a characteristic parameter for Pb^{3+} in a given coordination. This rule has been further supported by an ESR analysis of Pb^{3+} ions in the other ternary diamagnetic garnets $Y_3Al_5O_{12}$, $Lu_3Al_5O_{12}$, and $Lu_3Ga_5O_{12}$.

II. THEORY OF ESR SPECTRA

Among the stable isotopes of lead, Pb^{204} , Pb^{206} , and Pb^{208} have zero nuclear spin. Thus their ESR spectra will coincide and should consist of a single

somewhat unspecific line. Its g factor will be close to the free-spin value of 2.002, because of the dominant $6s$ character of the Pb^{3+} wave function. A weak anisotropy of the g factor must, in principle, be expected to occur because there are no sites in the garnet lattice which have perfect cubic symmetry. However, this effect was found to be too small to be detected experimentally, even at 35 GHz.³

Much more information about the local symmetry at a Pb^{3+} impurity site can be obtained from the anisotropy observed for the Pb^{207} hyperfine-structure satellites in the ESR spectra. We anticipate experimental results to be presented below and consider the local symmetry experienced by a Pb^{3+} ion at a dodecahedral c site, D_2 . Thus, the spin-Hamiltonian representative for trivalent Pb^{207} ions on the c sites in the garnet lattice reads

$$\mathcal{H}(\text{Pb}^{207}) = g\mu_B \vec{H} \cdot \vec{S} + \vec{I} \cdot \underline{A} \cdot \vec{S}, \quad (1)$$

with $\vec{I} \cdot \underline{A} \cdot \vec{S} = A_x I_x S_x + A_y I_y S_y + A_z I_z S_z$ and $I = S = \frac{1}{2}$.

The nuclear Zeeman interaction can be safely neglected in the present study. The local symmetry axes of the hyperfine-interaction tensor \underline{A} at a c site, x , y , z , must coincide with the crystallographic axes $\langle 110 \rangle$, $\langle 1\bar{1}0 \rangle$, and $\langle 001 \rangle$ of the cubic host. The hyperfine interaction can also be cast in the form

$$\vec{I} \cdot \underline{A} \cdot \vec{S} = A \vec{I} \cdot \vec{S} + \delta(3I_z S_z - \vec{I} \cdot \vec{S}) + \epsilon(I_x S_x + I_y S_y), \quad (2)$$

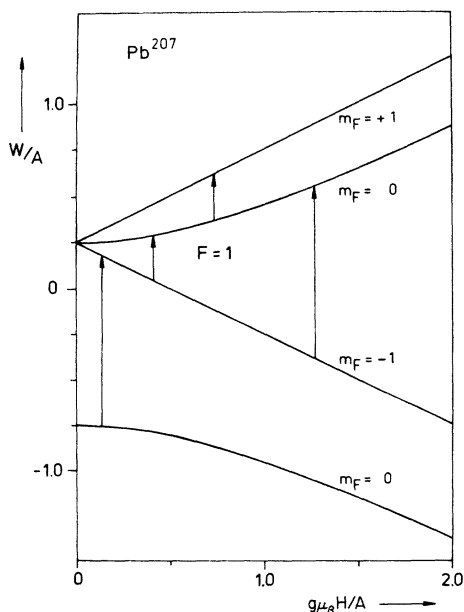


FIG. 1. Zeeman splitting of the electronic ground state of trivalent Pb^{207} in the isotropic Breit-Rabi limit. ESR transitions possible at 9.2 and 34.9 GHz in $\text{Y}_3\text{Ga}_5\text{O}_{12}$, where $A = 1.26 \text{ cm}^{-1}$, are indicated by short and long arrows.

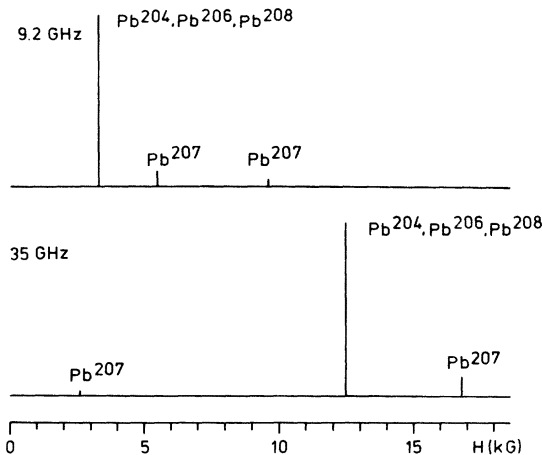


FIG. 2. Magnetic field positions and relative intensities of the Pb^{207} hyperfine-structure satellites in the ESR spectrum of Pb^{3+} in $\text{Y}_3\text{Ga}_5\text{O}_{12}$, at 9.2 and 34.9 GHz. A weak splitting of the Pb^{207} signals, which arises from the orthorhombicity of the A tensor, has been neglected.

with

$$A = \frac{1}{3}(A_x + A_y + A_z),$$

$$\delta = \frac{1}{2}(A_z - A), \quad \epsilon = \frac{1}{4}(A_x - A_y).$$

Effects resulting from an orthorhombicity of the hyperfine interaction are now better understood: Thus one notes that the $F=1$ zero-field triplet state will be split into three singlet states, and that a linear Zeeman effect is then no longer possible for any of the m_F -type sublevels.

Closed-form solutions of the Hamiltonian (1) still exist, if the static magnetic field \vec{H} is parallel to one of the principal axes of the hyperfine tensor, x , y or z .

For $\vec{H} \parallel z$ they read

$$W_{1,2} = \frac{1}{4}A_z \pm \left[\left(\frac{1}{2}g\mu_B H \right)^2 + \frac{1}{16}(A_x - A_y)^2 \right]^{1/2}, \quad (3)$$

$$W_{3,4} = \frac{1}{4}A_z \pm \left[\left(\frac{1}{2}g\mu_B H \right)^2 + \frac{1}{16}(A_x + A_y)^2 \right]^{1/2}.$$

The roots W_1 and W_2 correspond to the $F=1$ $m_F = \pm$ states of the isotropic Breit-Rabi case. The corresponding solutions for $\vec{H} \parallel x$ and $\vec{H} \parallel y$ are then obtained by cyclic permutation.

The Zeeman splitting of the electronic ground state of trivalent Pb^{207} is shown in Fig. 1, in the isotropic Breit-Rabi limit. This is a rather good approximation for the experimental situation encountered in the garnet lattice. The magnetically allowed dipole transitions, possible at 9 and 35 GHz, are indicated by arrows. In Fig. 2, the corresponding ESR spectra are schematically sketched.

III. EXPERIMENTAL PROCEDURE AND RESULTS

A. Crystal Growth

For the present study, nominally pure $\text{Y}_3\text{Ga}_5\text{O}_{12}$ single crystals were grown from high-temperature solution by a method previously reported for $\text{Y}_3\text{Fe}_5\text{O}_{12}$ single crystals,^{4,5} using the following melt composition (wt%): 39.33 PbO, 32.14 PbF_2 , 1.83 B_2O_3 , 0.03 CaO, 3.09 Ga_2O_3 , 9.90 Y_2O_3 , and 13.68 Ga_2O_3 . Y_2O_3 was a 99.999% grade of Mitsubishi; Ga_2O_3 was a 99.99% grade of Schuchardt (Ga 027) with Fe less than 1 ppm; PbO, B_2O_3 , and CaO (from CaCO_3) was a *pro analysi* quality of Merck with Fe less than 20 ppm; but the PbF_2 of Riedel de Haen had Fe about 100 ppm. The total melt was 1100 g; the slow cooling started at 1150 °C with 0.4 °C/h; and crystallization was stopped at 1060 °C by turning the crucible in the opposite position. The yield was 10 g consisting essentially of one crystal of 7.8 g, having very regular $\{211\}$ and $\{110\}$ facets and only one small flux inclusion. The color was light yellow. Chemical analysis of a part of this crystal showed 0.007 ± 0.001 Fe, 0.0040 ± 0.0005 Pb, and 0.003 ± 0.0001 F per formula unit, which was in good agreement to the results of crystals grown earlier from the same melt.

B. Electron-Spin Resonance

The ESR spectra were recorded on standard X-band and Q-band spectrometers. The dominant signals observed in our crystals arise from Fe^{3+} impurity ions residing on the octahedral sites in the garnet lattice. At a much higher level of detection, weak signals arising from the Fe^{3+} ions on the tetrahedral sites appear in the ESR spectrum. The ratio of Fe^{3+} ions occupying the tetrahedral *d* sites and the octahedral *a* sites could thus be estimated to be at least of the order of 1:25. This indicates a strong preference of the Fe^{3+} impurity ions for the octahedral sites in the garnet lattice. The effect appears to be more pronounced in flux-grown than in melt-grown garnet crystals, presumably because of the lower growth temperature of the former. The ESR spectra of Fe^{3+} impurity ions in melt-grown YGaG crystals have been thoroughly investigated by Geschwind.⁶

Upon rotating a $\text{Y}_3\text{Ga}_5\text{O}_{12}$ crystal around a $\langle 110 \rangle$ axis, the ESR signals arising from Fe^{3+} , and those of other transition-metal impurities, were found to be highly angular dependent in their magnetic-field position. In contrast, some rather weak, but in general angular-independent, ESR signals were detected. These will be attributed to Pb^{3+} impurity ions on the dodecahedral yttrium sites in the garnet lattice.

The strongest isotropic ESR signal arises from the zero-nuclear-spin isotopes; it occurs near the field position of the free-spin value. Thus

$$g(\text{Pb}^{3+}) = 2.002(2) .$$

The width of this signal amounted to about 50 G, at 300 K. No significant line narrowing was observed at lower temperatures. This linewidth therefore results from the nuclear moments of the ligands, especially from Ga^{69} and Ga^{71} .

At X-band frequencies, e.g., at 9.2 GHz, the first Pb^{207} satellite line occurs at 5.5 kG. It is angular independent, within the limits of experimental error, and corresponds to the $F=1$, $m_F = -1 \rightarrow F=1$, $m_F=0$ transition of the isotropic case (see Figs. 1 and 2). The other possible transition, $F=1$, $m_F=0 \rightarrow F=1$, $m_F=+1$, occurs at 9.5 kG, and shows a certain angular variation, and multiplicity. We will now demonstrate that this is a result of a slight orthorhombic distortion of the Pb^{207} hyperfine interaction tensor.

For a paramagnetic point defect which reflects the D_2 symmetry of the dodecahedral site in the garnet lattice, six magnetically different positions may be distinguished—for an arbitrary orientation of the static magnetic field \vec{H} . Upon rotating \vec{H} within a $\{110\}$ plane of the cubic crystal, only four ESR signals are expected to occur in the ESR spectrum. These will further coalesce into two signals for $\vec{H} \parallel \langle 100 \rangle$ and $\vec{H} \parallel \langle 111 \rangle$, and into three signals for $\vec{H} \parallel \langle 110 \rangle$. The corresponding ESR intensities for these orientations should be in the ratio 4:2, 3:3, and 4:1:1, respectively.⁷ This has been observed experimentally. The angular dependence of these four ESR signals, which arise from the $F=1$, $m_F=0 \rightarrow F=1$, $m_F=+1$ transition is shown in Fig. 3. The principal values of the hyperfine-interaction tensor were determined from the spectra $\vec{H} \parallel \langle 100 \rangle$ and $\vec{H} \parallel \langle 110 \rangle$ as

$$A_x = 37.8(6) \text{ GHz} = 1.263 \text{ cm}^{-1} ,$$

$$A_y = 37.9(8) \text{ GHz} = 1.267 \text{ cm}^{-1} ,$$

$$A_z = 37.7(9) \text{ GHz} = 1.261 \text{ cm}^{-1} .$$

Here the *z* axis is taken to be parallel to the $[001]$ direction, whereas *x* and *y* are defined along a pair of $[110]$ and $[\bar{1}\bar{1}0]$ axes. The data above were taken at 300 K. Their evaluation required numerical solutions of Eqs. (3), which were obtained by iteration. With the resulting principal values of the \underline{A} tensor, the angular dependence of the Pb^{207} hyperfine-structure satellites could be calculated by rigorous computer diagonalization of the 4×4 energy matrix.

The result of this numerical analysis is illustrated in Fig. 3 and is compared with the experimental data. The agreement is seen to be fair. Experimental errors arise from the considerable inhomogeneous linewidth of the ESR signals, and from a slight misorientation of the crystal. However, these data appear to be reliable enough to

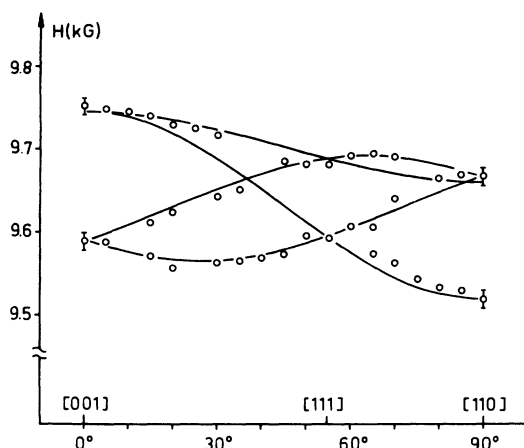


FIG. 3. Angular dependence of the $F=1$, $m_F=0 \rightarrow F=1$, $m_F=+1$ Pb^{207} hyperfine-structure satellites, upon rotating the magnetic field \vec{H} in a $\{110\}$ plane of the crystal at 9.2 GHz. The principal values of the hyperfine tensor result from extremal positions in the spectra $\vec{H} \parallel [001]$ and $\vec{H} \parallel [110]$. The solid lines were obtained by rigorous computer diagonalization of the 4×4 energy matrix.

demonstrate positively that the Pb^{3+} ions occupy the dodecahedral yttrium sites in the garnet lattice.

It should be mentioned that a corresponding computer analysis of the other Pb^{207} hyperfine-structure satellites predicted a much smaller angular variation. Thus, the isotropy of the Pb^{207} signal, observed at 5.5 kG for 9.2 GHz, and at 16.8 kG for 34.9 GHz, can be understood. The Q-band transition predicted to occur at 2.6 kG could not be positively identified because it strongly overlapped with the much more intensive Fe^{3+} signals.

IV. DISCUSSION

The occurrence of the trivalent charge state of lead on yttrium sites in $\text{Y}_3\text{Ga}_5\text{O}_{12}$ is not too surprising in view of the great chemical stability of the $5d^{10}6s^1$ configuration, which corresponds to that of the neutral gold atom. Consequently, Pb^{3+} ions might also be expected to be detectable by ESR in the other isomorphous diamagnetic garnet hosts, i.e., $\text{Y}_3\text{Al}_5\text{O}_{12}$, $\text{Lu}_3\text{Ga}_5\text{O}_{12}$, and $\text{Lu}_3\text{Al}_5\text{O}_{12}$. This was indeed found to be the case.⁸ Table I summarizes the experimental data. Also included are g -factor and Pb^{207} hyperfine-structure data previously reported for the Pb^{3+} ion in chemically quite different oxide hosts, such as ThO_2 , CeO_2 , CaWO_4 , CaO , and ZnO . Representative ESR data available for the Pb^{3+} ion in nonoxide anion ligand geometry, encountered in CaCO_3 , KCl , ZnSe , and ZnTe are also quoted.

In spite of the rather strong hyperfine interaction observed for the Pb^{3+} ion in solids, it should be remembered that the free-ion value⁹ A^{207}

= 2.60 cm^{-1} is still larger. This difference illustrates the fact that the wave function of a paramagnetic ion may undergo considerable delocalization, when incorporated in a solid. As pointed out by Watanabe,¹⁰ this effect is favored in the more covalent tetrahedrally coordinated hosts, as ZnO , ZnSe , and ZnTe . Simultaneously, the g factor is expected to increase, because a transfer of the unpaired spin to the nearest-neighbor anion shell represents a net hole transfer. Both effects are clearly indicated in Table I. Note that for the isoelectronic free gold atom¹¹ $g=2.0041$. The pronounced negative g shift observed for the Pb^{3+} ion in ThO_2 and CeO_2 may be a consequence of the rather large spin-orbit coupling constant of the next-nearest cation ligands.

The data in Table I also show that, within the class of diamagnetic garnet hosts, A^{207} decreases as their lattice constant a increases. A reduction of A^{207} is also indicated, as the number of nearest-

TABLE I. Compilation of g factor and Pb^{207} hyperfine-coupling data for Pb^{3+} impurity ions in solids. For those hosts, where the Pb^{3+} ion occupies sites of noncubic symmetry, g and A^{207} represent mean values. The number of nearest-neighbor anion ligands n and the garnet lattice constant a is also quoted.

Host	Ref.	g	A^{207} (cm^{-1})	n	a (\AA)
$\text{Y}_3\text{Ga}_5\text{O}_{12}$	a	2.002	1.264	8	12.28
$\text{Lu}_3\text{Ga}_5\text{O}_{12}$	a	2.001	1.272	8	12.19
$\text{Y}_3\text{Al}_5\text{O}_{12}$	a	2.002	1.339	8	12.00
$\text{Lu}_3\text{Al}_5\text{O}_{12}$	a	2.000	1.382	8	11.91
ThO_2	b	1.968	1.229	8	
CeO_2	c	1.965	1.20	8	
CaWO_4	d	1.990	1.277	8	
CaO	e	1.999	1.07	6	
ZnO	e	2.013	0.808	4	
CaCO_3	f	2.008	1.345	...	
KCl	g	2.034	1.101	6	
ZnSe	h	2.073	0.625	4	
ZnTe	i	2.167	0.523	4	

^aThis work.

^bReferences 1 and 2.

^cQuoted in Ref. 2.

^d A^{207} evaluated from experimental data given by G. Born, A. Hofstaetter, and A. Scharmann [Phys. Status Solidi **37**, 255 (1970)].

^eG. Born, A. Hofstaetter, and A. Scharmann, Phys. Lett. **36A**, 447 (1971).

^fR. M. Mineeva and L. V. Bershov, Fiz. Tverd. Tela [Sov. Phys.-Solid State **11**, 653 (1969)].

^gD. Schoemaker and J. L. Kolopus, Solid State Commun. **8**, 435 (1970).

^hK. Suto and M. Aoki, J. Phys. Soc. Jap. **26**, 287 (1969); W. C. Holton and R. K. Watts, J. Chem. Phys. **51**, 1615 (1969).

ⁱK. Suto and M. Aoki, J. Phys. Soc. Jap. **22**, 1307 (1967); **22**, 1517 (1967).

neighbor oxygen ligands, n , is lowered. These effects may be viewed as a consequence of the Pauli principle which restricts the spatial extension of the $6s$ orbital of Pb^{3+} , because of its overlap with the oxygen ligands. Thus, the nearest-neighbor oxygen shell will repel the $6s$ wave function and may contribute to an increased spin density at the central Pb^{207} nucleus. Mathematically, these effects result if the central $6s$ orbital is properly orthogonalized on the anion ligand wave functions. The weak anisotropy observed for the Pb^{207} hyperfine interaction in $\text{Y}_3\text{Ga}_5\text{O}_{12}$ can be accounted for by a small admixture of p or d character into the $6s$ ground-state wave function.

The question arises which percentage of the total lead impurity content can occur in the trivalent paramagnetic state. It must be expected that this fraction will change from sample to sample, depending on the exact growth conditions of the crystals. In our $\text{Y}_3\text{Ga}_5\text{O}_{12}$ samples, the total lead impurity concentration, as determined by atomic absorption, was 0.004 per formula unit. On the other hand, absolute ESR intensity measurements indicated that the Pb^{3+} concentration was of the same order of magnitude. In the other diamagnetic garnet crystals investigated, LuGaG , YAlG , and LuAlG , the Pb^{3+} concentration could be greatly enhanced by exposing the samples to ionizing radiation, as 50-keV x rays. Annealing in an oxidizing or reducing atmosphere should also change the valence state of lead. However, no systematic studies of such charge-transfer processes were undertaken so far.

It should also be mentioned that the more or less intense yellow coloration of PbO-PbF_2 flux-grown

diamagnetic garnet crystals appears to be correlated with the trivalent charge state of the lead impurity ions. The exact nature of the electronic transition responsible is not yet known.

The question remains whether lead impurity ions may also occur in the trivalent paramagnetic charge state, when present in a ferrimagnetic garnet, as $\text{Y}_3\text{Fe}_5\text{O}_{12}$. If so, one would not expect a serious influence on the magnetic properties of the host—because of the almost coinciding g factors of YIG and of the Pb^{3+} impurity, and because of the almost isotropic hyperfine interaction of the less-abundant Pb^{207} isotope. For the same reasons, no pronounced growth-induced magnetic anisotropy is expected to result from Pb^{3+} impurity ions, if site preference for some of the six equivalent c sites in the garnet lattice is energetically favored by the growth conditions of the crystal. Nevertheless, we have been unsuccessful in our attempts to detect a site selectivity for Pb^{3+} ions, and Fe^{3+} ions, in our flux-grown $\text{Y}_3\text{Ga}_5\text{O}_{12}$ crystals which had $\{110\}$ facets. The experimental conditions were the same as those described by Wolfe *et al.*¹² for Nd^{3+} and Yb^{3+} impurity ions in $\text{Y}_3\text{Al}_5\text{O}_{12}$. Here, a strong site selectivity of the $4f$ impurity ions was unambiguously established.

ACKNOWLEDGMENTS

The authors wish to thank R. Röhrig for his help in the evaluation of the ESR spectra, and O. Schirmer for illuminating discussions. The authors also gratefully acknowledge the valuable assistance of several technical staff members at the Philips Forschungslaboratorium, Hamburg.

¹R. Röhrig and J. Schneider, Phys. Lett. 30A, 371 (1969).

²J. L. Kolopus, C. B. Finch, and M. M. Abraham, Phys. Rev. B 2, 2040 (1970).

³A weak trigonal anisotropy of the g factor could be detected in ThO_2 , for those Pb^{3+} ions which are associated with a charge-compensating fluorine impurity replacing a nearest-neighbor oxygen ligand (see Refs. 1 and 2).

⁴W. Tolksdorf, J. Cryst. Growth 3/4, 463 (1968).

⁵W. Tolksdorf and F. Welz, J. Cryst. Growth 13/14, 566 (1972).

⁶S. Geschwind, Phys. Rev. 121, 363 (1961).

⁷It is here tacitly assumed that the distribution of Pb^{3+} ions over the different sites in the garnet lattice is uniform. This must not be necessarily so since, during the growth of the

crystal, a preference for a particular yttrium site is possible (see Ref. 12).

⁸Single crystals of these materials were kindly made available to us by Professor B. Elschner, Darmstadt. They were also grown from a PbO-PbF_2 based flux. A determination of the anisotropy of the hyperfine interaction was not attempted.

⁹A. L. Schawlow, J. N. P. Hume, and M. F. Crawford, Phys. Rev. 76, 1876 (1949).

¹⁰H. Watanabe, Phys. Rev. 149, 402 (1966).

¹¹N. F. Ramsey, *Molecular Beams* (Clarendon, Oxford, England, 1956).

¹²R. Wolfe, M. D. Sturge, F. R. Merritt, and L. G. Van Uitert, Phys. Rev. Lett. 26, 1570 (1971).